Korean J. Chem. Eng., 37(12), 2209-2215 (2020)
DOI: 10.1007/s11814-020-0668-1

pISSN: 0256-1115
eISSN: 1975-7220

A functionalized nanocomposite adsorbent for the sequential removal of radioactive iodine and cobalt ions in aqueous media

Jung Eun Park*,‡, Ha Eun Shim,‡, Sajid Mushtaq***, Yong Jun Choi****, and Jongho Jeon*,†**

*Department of Applied Chemistry, School of Applied Chemical Engineering, Kyungpook National University, Daegu 41566, Korea
**Advanced Radiation Technology Institute, Korea Atomic Energy Research Institute, Jeongeup 56212, Korea
***Department of Nuclear Engineering, Pakistan Institute of Engineering and Applied Sciences, Islamabad, 45650, Pakistan
****School of Environmental Engineering, University of Seoul, Seoul 02504, Korea
(*Received 24 June 2020 • Revised 20 August 2020 • Accepted 26 August 2020*)

Abstract−The need for efficient remediation of the radioactive waste caused by undesirable nuclear accidents and overspending of radionuclides has gained worldwide attention, with extensive recent efforts made to protect the environment from radioactive contamination. Although various treatment processes for the removal of radionuclides and the purification of liquid waste have been reported, the development of a better decontamination method is still necessary for obtaining enhanced desalination performances. Herein, we report a dual-functional composite adsorbent composed of a cellulose acetate membrane as a solid support, gold nanoparticles (AuNPs), and a metal chelating agent which can potentially be used to efficiently remove radioactive iodine and cobalt. In the desalination experiments, the sorption membrane was able to remove cobalt ions rapidly in water. Isotherm data shows that approximately 180 Co^{2+} atoms were captured per AuNP. Next, the same material was used for the adsorption of iodide anions. Within a few minutes, more than 99% of radioactive iodine was removed even in the presence of other ion species. These findings clearly demonstrate that the desalination method presented in here provides a useful approach for the sequential removal of toxic metal and halogen species in aqueous media.

Keywords: Desalination, Composite Materials, Nanoadsorbents, Radioactive Wastes, Adsorption

INTRODUCTION

Nuclear energy has been recognized as an excellent alternative to conventional, carbon-based energy resources to sustainably meet world energy demands. However, the extensive utilization of nuclear power plants and other applications, such as the development of nuclear weapons and various biomedical uses, the remediation of radioactive and nuclear wastes is an important issue as environmental exposure of radioactive contaminants can result in significant public health hazards [1-3]. In addition, dramatic nuclear accidents such as Chernobyl in 1986 and Fukushima in 2011 caused the release of dangerous radionuclides into the environment. Most of these elements, including ^{60}Co, ^{90}Sr, ^{99}Tc, ^{134}Cs, ^{137}Cs, ^{129}I and ^{131}I, possess long decay half-lives, high water solubility, and high level of ionizing energy emissions [4,5]. Therefore, even trace amounts of radionuclides in aqueous media can result in long-term radiological toxicity for ecosystem and human health. Among the various radioisotopes, radioactive iodine (e.g., ^{129}I, ^{131}I), a fission product, is believed to be one of the most hazardous elements released in nuclear plant accidents and has been extensively used in biomedical applications, meaning that liquid waste containing radioactive iodines (^{124}I, ^{125}I, ^{131}I) is discharged by many medical institutions [6,7]. In addition, radioactive cobalt (^{60}Co) is typically produced as a by-product from the neutron activation of iron isotopes in the reactor's steel structures during nuclear power plant operation [8]. It is also a target species that must be removed during the maintenance or decommissioning of nuclear reactors. Moreover, radioactive cobalt is widely utilized as a useful radiation source in several industrial applications that include security screenings, sterilization, food irradiation, and radiation therapy [9,10]. The wide use of such radionuclides requires efficient decontamination processes for managing radioactive waste.

Previously, we reported that gold nanoparticles (AuNPs) immobilized on a polymeric matrix are an excellent sorbent for remediating radioactive iodines [11-14]. Using the developed system, the ion-selective capture of radioactive iodine was achieved in various aqueous solutions. Although these methods showed superior results when compared to previous experiments, their application was limited to removing halogen species (iodide anion). The development of more cost-effective and efficient remediation procedures for a broad range of radionuclide is still necessary. We hypothesized that the surface of AuNPs could be modified by specific ligands and allow for the incorporation of a suitable molecule to increase the functionality of the sorption material [15,16]. In this study, we demonstrate a useful new method for removing both iodide and cobalt in water by incorporating a metal chelator into the nanocomposite membrane, which can adsorb iodide anions and rapidly trap cobalt cations.

†To whom correspondence should be addressed.
E-mail: jeonj@knu.ac.kr
‡These authors contributed equally to this work.

MATERIALS AND METHODS

1. General Methods

Chloroauric acid trihydrate ($HAuCl_4 \cdot 3H_2O$), sodium citrate tribasic dihydrate, cobalt(II) chloride, xylenol orange, aqueous hydrochloric acid, and nitric acid were purchased from Sigma Aldrich Korea. Dithiobis (C_2-NTA, NTA-SH) was purchased from Dojindo Molecular Technologies, Inc. Cellulose acetate membranes (CAM, pore size=0.20 μm, diameter=47 mm) were purchased from Advantec MFS. [^{125}I]NaI was supplied by New Korea Industrial Co. Ltd. The radioactivity of [^{125}I]NaI was measured by using a radioactivity dose calibrator (Capintec, Inc) and γ-counter (PerkimElmer, 2480 Automatic gamma counter). Removal efficiency of the [^{125}I]NaI by Au-DC was determined with a γ-counter (PerkimElmer, 2480 Automatic gamma counter). The elemental composition of the gold nanomaterials was analyzed by SEM-energy-dispersive X-ray (EDX) (EDAX Apollo XL, AMETEK, Mahwah, NJ, USA) analysis with accelerating voltages of 20 kV. EDX spectra were recorded in area scanning mode by focusing the electron beam onto a region of the sample surface.

2. Synthesis of Citrate-stabilized Gold Nanoparticles (AuNPs)

All glassware was washed using aqua regia, a mixture of three parts hydrochloric acid and one part nitric acid by volume. A solution of chloroauric acid (1 mM, 150 mL) was heated to reflux and a solution of sodium citrate tribasic dihydrate (38.8 mM, 15 mL) was quickly added to the mixture. The resulting solution was stirred for 15 min to allow the full reduction of the gold salt. The deep red-colored suspension was then cooled to room temperature. The concentration of AuNPs was measured by UV-vis spectroscopy (concentration=1.0×10^{-8} M with an extinction coefficient of 2.8×10^8 at 520 nm with a 1 cm path length). The AuNPs solutions were stored in dark glass bottles at 4 °C.

3. Preparation of the Gold Nanoparticle-immobilized Cellulose Acetate Membrane (Au-CAM)

Au-CAM were prepared following a previously reported procedure [12]. Briefly, a glass vacuum filter assembly was used to manufacture Au-CAM (pore size=0.20 μm, diameter=47 mm). A CAM was placed between the filter holder fritted glass support and a graduated funnel (Fig. S3). Citrate-stabilized AuNPs (10 mL, 10 nM) were poured into the graduated funnel and then a vacuum was applied until all the nanoparticles passed through the membrane. The membrane was washed with deionized water several times before the same procedure using AuNPs (10 mL, 10 nM) was conducted on its opposite side. The Au-CAM was kept under ambient conditions until its application in the desalination experiment.

4. Preparation of Metal Chelator-loaded Au-CAM (NTA-Au-CAM)

A solution of 3,3′-Dithiobis[N-(5-amino-5-carboxypentyl)propionamide-N,N′-diacetic acid] (NTA-disulfide) (20 μM, 2.5 mL) was added to the Au-CAM in a petri dish (50 mm diameter×15 mm height). It was then shaken gently at room temperature overnight. After the incorporation of the chelator onto the membrane, the NTA-Au-CAM was rinsed with deionized water several times.

5. Removal of Cobalt Ions using NTA-Au-CAM

To measure the amount of Co^{2+} ions captured on NTA-Au-CAM, an aqueous solution of $CoCl_2$ (2.5-100 μM, 3 mL) was added to the membrane. NTA-Au-CAM, with a AuNP region diameter of 36 mm, was immersed in the $CoCl_2$ solution and gently shaken at room temperature. At specific time points (1, 3, 5, 10, 30 and 60 min post incubation of the NTA-Au-CAM), the supernatant (50 μL) was collected and mixed with the same volume of a xylenol orange stock solution. The concentration of cobalt ions remaining in the solution was measured using the absorbance ratio of the solution at 430 and 580 nm (Fig. S1).

6. Removal of Iodide Ions using NTA-Au-CAM

To measure the adsorption efficiency of I^- ions by NTA-Au-CAM, an aqueous solution of NaI (10-500 μM, 3 mL) was added to the membrane. NTA-Au-CAM, with a AuNP region diameter of 36 mm, was immersed in the NaI solution and gently shaken at room temperature. At given time points (1, 3, 5, 10 and 30 min post incubation of the NTA-Au-CAM), the solution (50 μL) was collected and the iodide ion concentration of the solution was determined by UV-vis spectroscopy (the absorbance intensity at 218 nm) (Fig. S2).

7. Removal of Radioactive Iodine ($^{125}I^-$) using Nanocomposite Membranes

To investigate the performance of the NTA-Au-CAM for the desalination of radioactive iodine, [^{125}I]NaI (3.7-74 MBq) was diluted with 3 mL of various aqueous media and poured into petri dishes (50 mm diameter×15 mm height). NTA-Au-CAM, with a AuNP region diameter of 36 mm, was immersed in each petri dish and kept at room temperature under gentle shaking. At given time points (1, 3, 5, 10, 30 and 60 min post incubation of NTA-Au-CAM), the solution (10 μL) was collected and the radioactivity of the solution was measured using a γ-counter.

RESULTS AND DISCUSSION

The preparation of the functionalized nanocomposite material (NTA-Au-CAM) for desalination experiments is shown in Fig. 1(a). First, the immobilization of the citrate-stabilized AuNPs was carried out using a commercially available CAM. The as-prepared AuNPs (mean diameter=13 nm, 100 pmol) were passed through the membrane (0.20 μm pore size, 47 mm diameter) under reduced pressure to create the AuNPs-embedded cellulose acetate membrane (Au-CAM), which exhibited a homogeneous and deep red-violet color (Fig. S3). Using a vacuum filter system, nanomaterials can be incarcerated on both sides of the CAM, immobilizing 200 pmol of nanoparticles on the membrane. The nanomaterials deposited on the membrane neither washed out in various aqueous solutions (e.g. 0.1 M HCl, 0.1 M NaOH, 1.0 M NaCl) nor lost their stability and chemical properties even after drying for several weeks, suggesting that this simple procedure allows for the quick fabrication of Au-CAM (Fig. S4). Scanning electron microscopy (SEM) analysis clearly showed many AuNPs distributed on the cellulose acetate nanofibers, which exhibited a porous and rough surface (Fig. 1(c)). The formation of stable composite materials could be rationalized by the large number of carbonyl and hydroxy groups, which possess lone pair electrons, in the cellulose acetate that could act as anchor points for immobilizing nanoparticles, as such electrostatic interactions or complexation would result in the immobilization of AuNPs while preventing aggregation [17]. Next, a metal chelator

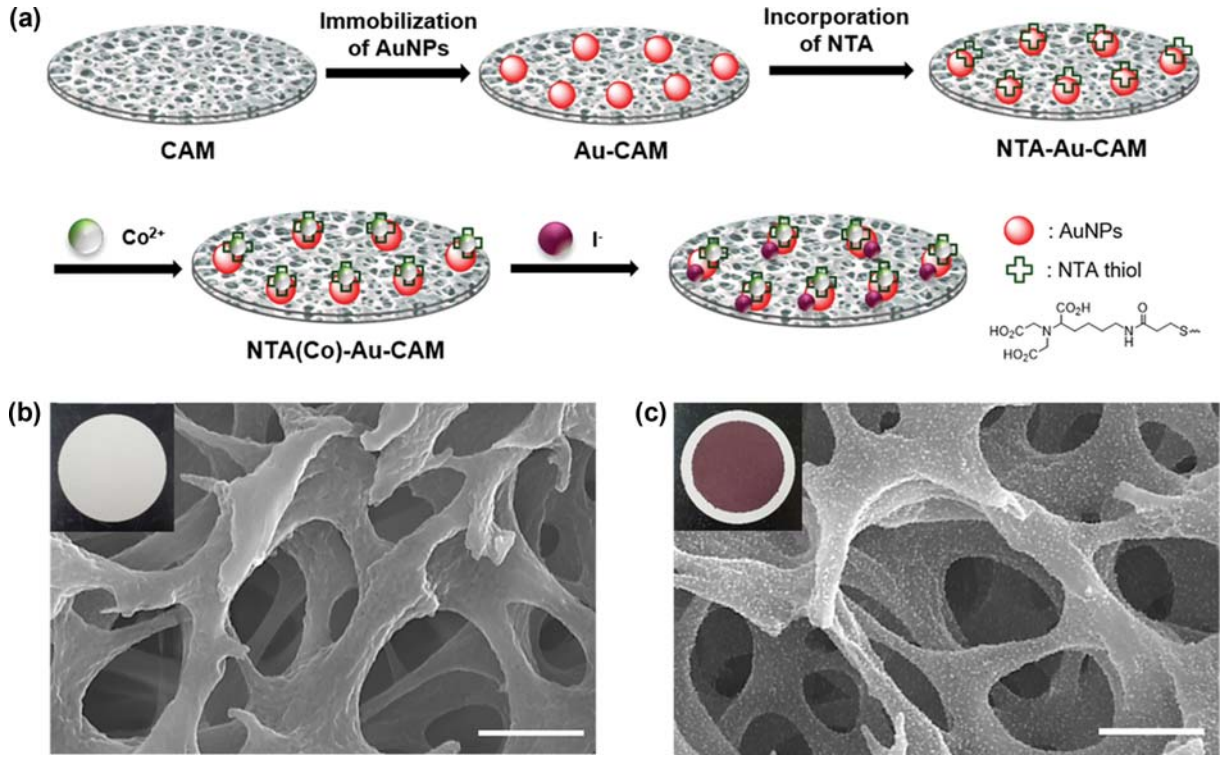

Fig. 1. (a) Preparation of NTA-Au-CAM and its application for the desalination of cobalt and iodide ions in water. Scanning electron microscopy (SEM) images of (b) CAM and (c) NTA-Au-CAM (Scale bar=500 nm), White dots show AuNPs deposited on the membrane.

(a)

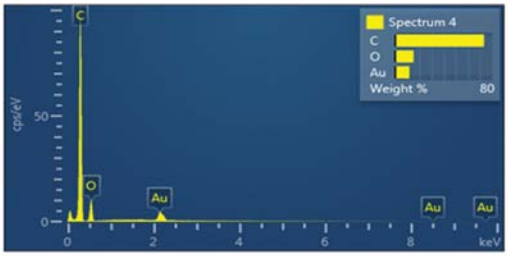

Element	Wt%	Atomic %
C	73.18	85.87
O	15.10	13.30
Au	11.72	0.84
Total:	100.00	100.00

(b)

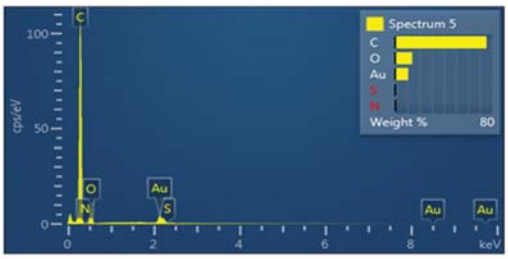

Element	Wt%	Atomic %
C	75.24	87.04
O	14.00	12.16
S	0.13	0.06
Au	10.63	0.75
Total:	100.00	100.00

(c)

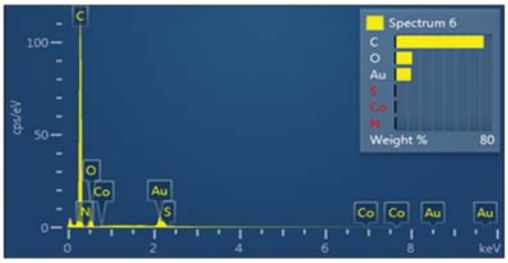

Element	Wt%	Atomic %
C	72.96	86.62
O	13.90	12.39
S	0.09	0.04
Co	0.05	0.01
Au	13.00	0.94
Total:	100.00	100.00

Fig. 2. Energy-dispersive X-ray spectroscopy (EDX) analysis of (a) Au-CAM, (b) NTA-Au-CAM, and (c) Co^{2+} captured NTA-Au-CAM [NTA(Co)-Au-CAM].

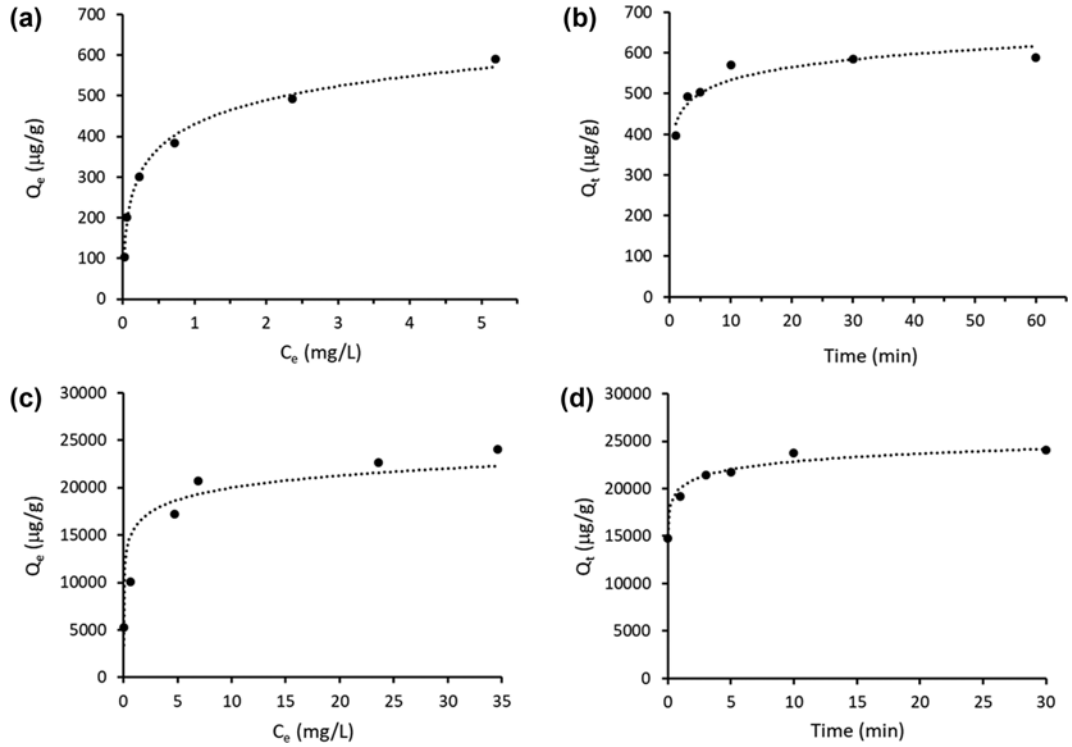

Fig. 3. Desalination performance of the composite adsorbent. Isotherm data for Co^{2+} and I^- ((a) and (c) respectively); kinetic sorption data for Co^{2+} (100 mM) and I^- (500 mM) ((b) and (d), respectively).

was attached to the surface of nanoparticles through gold-thiol bonding. We selected the thiol group bearing nitrilotriacetic acid (NTA) as the chelating agent for this study as it has been used for functionalized gold surfaces for various biochemical applications. Previous studies reported that the tetradentate NTA ligand forms a stable complex with metal (II) ions, and we hypothesized that the NTA on the Au-CAM would be capable of chelating cobalt ions in aqueous media [18-20]. The sorption material can simultaneously remove iodide anions using the surface of the AuNPs while the chelator is active (Fig. 1(a)). To prepare the NTA-incorporated Au-CAM (NTA-Au-CAM), a thiolated NTA solution was added to Au-CAM. The resulting membrane was shaken for 12 h at room temperature and then washed several times with deionized water. Elemental analysis of NTA-Au-CAM using energy-dispersive X-ray spectroscopy (EDX) showed a set of peaks representing gold atoms and sulfur atoms, representing the incorporation of the nanomaterials and chelators on the membrane (Fig. 2(a) and 2(b)). Other elements, such as carbon and oxygen atoms, were observed and attributed to the carbohydrates of the cellulose acetate polymers. These results demonstrate that NTA-Au-CAM was successfully prepared and ready for further study.

To investigate the desalination capability of the composite membrane, NTA-Au-CAM was first immersed in aqueous solutions containing $CoCl_2$. Fig. 3(a) presents the typical desalination performance of NTA-Au-CAM for Co^{2+} with a contact time of 30 min. The removal capacity (Q_e) of the composite adsorbent increased with an increase in the initial concentration of Co^{2+}. The chelation of Co^{2+} was also confirmed by the result of EDX analysis that shows a characteristic Co peak (Fig. 2(c)). The linear fitting of the observed data based on Langmuir and Freundlich isotherm models (Fig. S5) revealed that NTA-Au-CAM was better estimated by the Langmuir equation with a correlation factor (R^2) of 0.992. The corresponding parameters for these models are summarized in Table 1. In addition, we conducted the same desalination experiments in the presence of other ions and under different pH conditions. As shown in Fig. 4, the removal efficiency was slightly reduced in 100 mM NaCl and basic media, but the efficiency of cobalt chelation of cobalt dramatically decreased under acidic conditions. This is likely because the chelator is protonated under low pH and cannot effectively capture metal ions compared to its deprotonated forms. The adsorption kinetic parameters are also key factors for the practical application of the composite adsorbent.

Table 1. Isotherm parameters for the removal of Co^{2+} and I^-

Ion	Langmuir constants			Freundlich constants		
	K_L (L mg^{-1})	Q_{max} (mg g^{-1})	R^2	K_F (mg g^{-1}) (L mg^{-1})$^{1/n}$	n	R^2
Co^{2+}	4.043	0.601	0.992	0.399	3.413	0.936
I^-	0.969	24.3	0.997	13.7	6.527	0.956

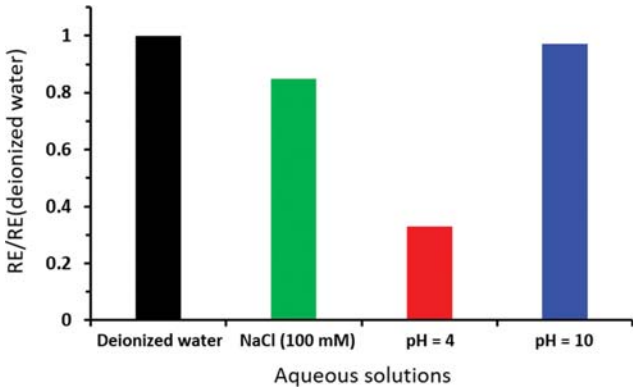

Fig. 4. Comparison of removal efficiencies [RE: removal efficiency in aqueous solutions, RE (deionized water): removal efficiency in deionized water].

The removal efficiency of Co^{2+} was measured as a function of time (1-60 min) to determine an optimum time for the desalination experiments (Fig. 3(b)). The removal of Co^{2+} was rapid in the first 10 min before reaching an equilibrium by 30 min. The fitting results of the pseudo-first and pseudo-second-order kinetic models are shown in Fig. S6 and Table 2. Based on the calculated kinetic parameters, it is clear that the pseudo-second kinetic model fits better with the kinetic results.

We next investigated the adsorption of iodide ions using the cobalt ion-captured membrane (NTA(Co)-Au-CAM) to explore the sequential removal of two different ions with a single sortion material. After the finishing of the chelation of cobalt ions, the membrane was then immersed in an iodide solution. Fig. 3(c) and Table 1 show the isotherm parameters that indicate that the calculated maximum adsorption capacity (Q_{max}) from the Langmuir model is 24.3 mg/g. The kinetic curve is shown in Fig. 3(d). The adsorption of I^- is very rapid in the first 3 min, then slows, and finally reaches a plateau after 10 min. The corresponding kinetic parameters and correlation coefficients are listed in Table 2, which exhibits an R^2 value of the pseudo-second-order model that is closer to 1, higher than that of the pseudo-first-order model. In addition, the theoretical Q_{max} for I^- obtained from the pseudo-second-order model is closer to the experimental Q_{max} value. These results indicate

Table 2. Kinetic parameters for the removal of Co^{2+} and I^-

Ion	Experimental value	Pseudo-first order			Pseudo-second order		
	$Q_{e,exp}$ (mg g^{-1})	k_1 (min^{-1})	$Q_{e,cal}$ (mg g^{-1})	R^2	k_2 (g mg^{-1} min^{-1})	$Q_{e,cal}$ (mg g^{-1})	R^2
Co^{2+}	0.591	0.0965	0.394	0.952	2.72	0.596	0.999
I^-	24.1	0.6203	6.73	0.992	0.145	24.3	0.999

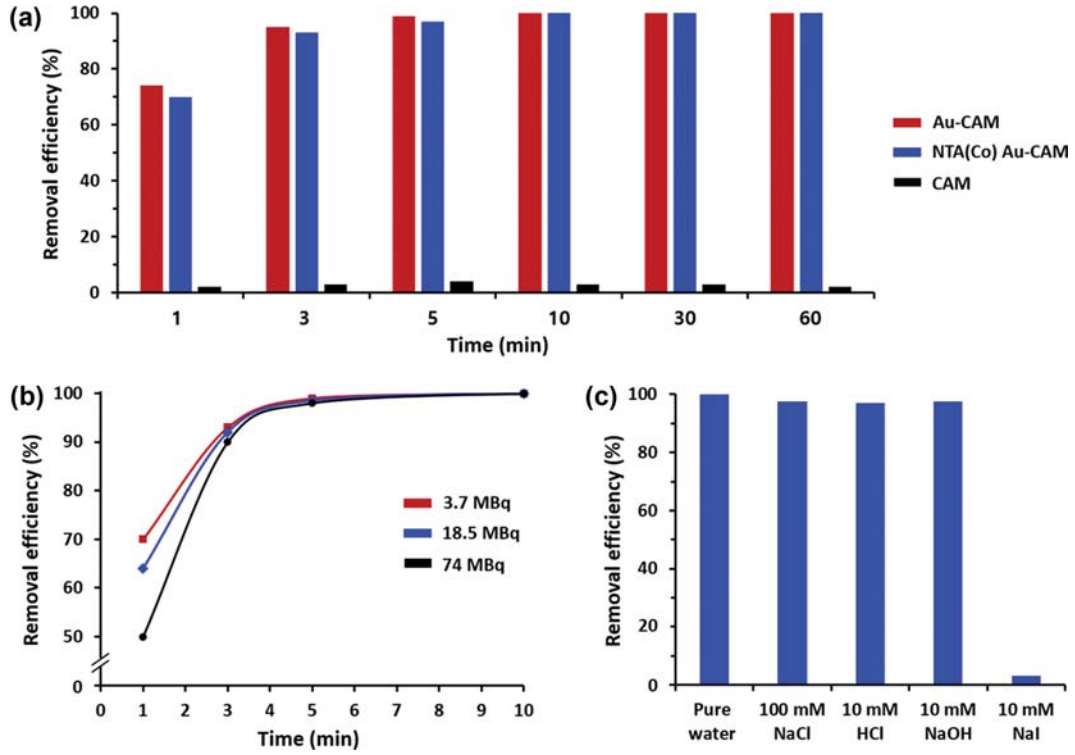

Fig. 5. (a) Time-dependent desalination efficiency of radioactive iodine ([^{125}I]NaI, 3.7 MBq/3 mL pure water) using Au-CAM and NTA(Co)-Au-CAM for 60 min. (b) Effect of the amount of radioactive iodine on the removal efficiency. (c) Effects of other ions in aqueous solutions and pH conditions on the removal efficiencies of radioactive iodine using NTA(Co)-Au-CAM.

that the adsorption behavior of both Co^{2+} and I^- is well described by the pseudo-second-order kinetics, suggesting that the rate-limiting step is surface adsorption and involves chemiadsorption.

Finally, we applied the composite adsorbent to the desalination of radioactive iodine. For this experiment, both Au-CAM and NTA(Co)-Au-CAM were immersed in aqueous solutions containing 3.7 MBq of [^{125}I]NaI, equivalent to ca. 5 pmol of radioactive iodine. As shown in Fig. 5(a), more than 95% of the radioactivity rapidly adsorbed onto the composite membranes. After just 10 min of incubation, less than 0.5% of the [^{125}I]NaI was detected in the water, with desorption of the iodide anions from the adsorbents not observed for several hours. In contrast, the non-modified CAM could not capture the radioactive iodide under the same experimental conditions. For the first 10 min the removal efficiency of the NTA(Co)-Au-CAM was slightly lower than the Au-CAM, which does not contain the NTA-thiol ligands on the surface. The desalination efficiency was also evaluated with different amount of radioactive iodine, varying from 3.7 to 74 MBq. Fig. 5(b) shows that the initial adsorption kinetics (<3 min) were slower at higher concentrations of [^{125}I]NaI. Within 5 min, most of the iodide anions were rapidly captured by the composite membrane (NTA(Co)-Au-CAM) and giving a removal efficiency of over 99%. After the desalination was accomplished, the radioactive iodines-adsorbed membrane could easily be removed from the water. The radioactivity quantification by a γ-counter showed that the radioactive iodine initially detected in water was transferred to the membrane. More importantly, these high removal efficiencies were also observed in the presence of other ions and under different pH conditions (Fig. 5(c)). For example, an excellent removal efficiency was still achieved in a 100 mM NaCl solution, which contains orders of magnitude more chloride ions than iodide ions ($[Cl^-]/[I^-]=>10^7$). The adsorption of radioactive iodine was completely inhibited by the presence of excess non-radioactive NaI (10 mM), likely due to the occupation of the adsorbent surface by the large amount of non-radioactive iodide ions ($^{127}I^-$). Taken together, these results clearly demonstrate that NTA-Au-CAM enables sequential removal of cobalt and radioactive iodine ions with rapid adsorption kinetics.

Until now, a variety of nanocomposite materials with unique physical and chemical properties including large surface area, specific reactivity, and selectivity toward target species have been developed as potential adsorbents for the efficient decontamination of radionuclides in aqueous media [21,22]. Some of these materials have been designed to possess multiple functions and have been applied to remove two different hazardous elements using mechanisms like chemisorption, complexation, ion change, and surface precipitation [23-31]. However, most of these methods require additional steps to separate the unsettled adsorbents from the water following the desalination procedure. Moreover, nano- or micro-sized sorbents tend to easily aggregate under certain conditions, including high salt concentrations, which results in the loss of their physicochemical properties. The composite membrane in this study is an alternative method that addresses the above-mentioned demerits as it can maintain the stability of the adsorbents during the decontamination process under various conditions while offering easy isolation of the radioactive element-adsorbed materials without requiring further separation processes. The NTA-Au-CAM used in the desalination experiments shows rapid adsorption kinetics for radioactive iodide anions with excellent removal efficiency. Given that the present method provides an excellent removal efficiency of more than two orders of magnitude in a mixed aqueous medium, composite membrane-based desalination is a promising process for treating the radioactive iodine waste generated by medical and industrial applications. The same sorbent also exhibited rapid removal of cobalt ions with a maximum adsorption capacity of 0.6 mg/g, equivalent to ca. 180 cobalt atom per AuNPs. The use of a polymeric ligand that contains multiple metal chelating agents or the application of a modified chelator that can more specifically remove the target ions could further improve the removal efficiency of the membrane. It is widely known that a variety of functionalized molecules bearing a thiol group or organic-inorganic composites can be introduced to the surface of AuNPs. This current methodology is not limited to the desalination of toxic metal and halogen species, but can be a useful platform for the removal of other hazardous materials by incorporating specific ligands into the composite membrane.

CONCLUSION

We demonstrated a novel desalination process using an engineered membrane capable of removing two different ions from aqueous media. Au-CAM was simply functionalized using a thiolated metal chelator, generating NTA-Au-CAM. The composite membrane is highly stable in aqueous solutions containing high concentrations of salts and over a range of pH values. Using this sorbent material, cobalt ions and iodide anions were efficiently captured by the NTA and AuNP surfaces, respectively. The experimental data showed the rapid removal of both ions, which can be described by a pseudo-second-order kinetic model and the Langmuir isotherm model. As the thin-layered composite material in this study provided rapid removal performance, NTA-Au-CAM can be applied in membrane filter system for the continuous inflow desalination of radioactive elements in aqueous media.

ACKNOWLEDGEMENTS

This research was funded by the National Research Foundation of Korea (Grant number: 2019R1F1A1061596).

SUPPORTING INFORMATION

Additional information as noted in the text. This information is available via the Internet at http://www.springer.com/chemistry/journal/11814.

REFERENCES

1. M. V. Ramana, *Wires Energy Environ.*, **7**, e289 (2018).
2. International Atomic Energy Agency, *IAEA/NSR* (2019).
3. M. Khayet and T. Matsuura, *Desalination*, **321**, 1 (2013).
4. A. Lerebours, D. Gudkov, L. Nagorskaya, A. Kaglyan, V. Rizewski, A. Leshchenko, E. H. Bailey, A. Bakir, S. Ovsyanikova, G. Laptev and J. T. Smith, *Environ. Sci. Technol.*, **52**, 9442 (2018).

5. N. S. Fisher, K. Beaugelin-Seiller, T. G. Hinton, Z. Baumann, D. J. Madigan and J. Garnier-Laplace, *Proc. Natl. Acad. Sci. U.S.A.*, **110**, 10670 (2013).
6. X. Hou, P. P. Povinec, L. Zhang, K. Shi, D. Biddulph, C.-C. Chang, Y. Fan, R. Golser, Y. Hou, M. Ješkovský, A. J. T. Jull, Q. Liu, M. Luo, P. Steier and W. Zhou, *Environ. Sci. Technol.*, **47**, 3091 (2013).
7. R. Ravichandran, *Management of radioactive wastes in a hospital environment*, Springer, Publications, Singapore (2017).
8. D. Kontogeorgakos, F. Tzika and I. E. Stamatelatos, *Nucl. Technol.*, **175**, 435 (2017).
9. D.-Q. Luo, S.-S. Zhao, Y.-R. Tang, Q.-J. Wang, H.-J. Liu and S.-C. Ma, *J. Anal. Methods Chem.*, **8**, 1 (2018).
10. C. Joshi, S. Dhanesar, J. Darko, A. Kerr, P. Vidyasagar and L. Schreiner, *J. Med. Phys.*, **34**, 137 (2009).
11. H. E. Shim, S. Mushtaq and J. Jeon, *J. Vis. Exp.*, **137**, e58105 (2018).
12. S. Mushtaq, S.-J. Yun, J. E. Yang, S.-W. Jeong, H. E. Shim, M. H. Choi, S. H. Park, Y. J. Choi and J. Jeon, *Environ. Sci. Nano*, **4**, 2157 (2017).
13. M. H. Choi, S.-W. Jeong, H. E. Shim, S.-J. Yun, S. Mushtaq, D. S. Choi, B.-S. Jang, J. E. Yang, Y. J. Choi and J. Jeon, *Chem. Commun.*, **53**, 3937 (2017).
14. M. H. Choi, H. E. Shim, S.-J. Yun, S. H. Park, D. S. Choi, B.-S. Jang, Y. J. Choi and J. Jeon, *ACS Appl. Mater. Interfaces*, **8**, 29227 (2016).
15. Q. Ong, Z. Luo and F. Stellacci, *Acc. Chem. Res.*, **50**, 1911 (2017).
16. N. Elahi, M. Kamali and M. H. Baghersad, *Talanta*, **184**, 537 (2018).
17. M. Kaushik and A. Moores, *Green Chem.*, **18**, 622 (2016).
18. S. V. Wegner and J. P. Spartz, *Angew. Chem.*, **52**, 7593 (2013).
19. T. T. Le, C. P. Wilde, N. Grossman and A. E. G. Cass, *Phys. Chem. Chem. Phys.*, **13**, 5271 (2011).
20. J. F. Hainfeld, W. Liu, C. M. R. Halsey, P. Freimuth and R. D. Powell, *J. Struct. Biol.*, **127**, 185 (1999).
21. L. R. Khanal, J. A. Sundararajan and Y. Qiang, *Energy Technol.*, **8**, 1901070 (2020).
22. Y. Yuan, H. Wang, S. Hou and D. Xia, *Wiley-VCH: Hoboken*, Publications, USA (2018).
23. X. Zhang and Y. Liu, *Environ. Sci. Nano*, **7**, 1008 (2020).
24. W. Song, X. Wang, Q. Wang, D. Shao and X. Wang, *Phys. Chem. Chem. Phys.*, **17**, 398 (2015).
25. M. E. Mahmoud, E. A. Saad, M. A. Soliman and M. S. Abdelwahab, *RSC Adv.*, **6**, 66242 (2016).
26. E. H. Borai, M. M. E. Breky, M. S. Sayed and M. M. Abo-Aly, *J. Colloid Interface Sci.*, **450**, 17 (2015).
27. D. Yang, S. Sarina, H. Zhu, H. Liu, Z. Zheng, M. Xie, S. V. Smith and S. Komarneni, *Angew. Chem. Int. Ed.*, **50**, 10594 (2011).
28. Y.-Y. Chen, S.-H. Yu, Q.-Z. Yao, S.-Q. Fu and G.-T. Zhou, *J. Colloid Interface Sci.*, **510**, 280 (2018).
29. M. F. Attallah, A. I. Abd-Elhamid, I. M. Ahmed and H. F. Aly, *J. Mol. Liq.*, **261**, 379 (2018).
30. C. Xiao, Z. H. Fard, D. Sarma, T.-B. Song, C. Xu and M. G. Kanatzidis, *J. Am. Chem. Soc.*, **139**, 16494 (2017).
31. M. E. Mahmoud, E. A. Allam, E. A. Saad, A. M. El-Khatib and M. A. Soliman, *J. Polym. Environ.*, **27**, 421 (2019).

Supporting Information

A functionalized nanocomposite adsorbent for the sequential removal of radioactive iodine and cobalt ions in aqueous media

Jung Eun Park[*,‡], Ha Eun Shim[,‡], Sajid Mushtaq[***], Yong Jun Choi[****], and Jongho Jeon[*,†]**

*Department of Applied Chemistry, School of Applied Chemical Engineering,
Kyungpook National University, Daegu 41566, Korea
**Advanced Radiation Technology Institute, Korea Atomic Energy Research Institute, Jeongeup 56212, Korea
***Department of Nuclear Engineering, Pakistan Institute of Engineering and Applied Sciences, Islamabad, 45650, Pakistan
****School of Environmental Engineering, University of Seoul, Seoul 02504, Korea
(*Received 24 June 2020 • Revised 20 August 2020 • Accepted 26 August 2020*)

1. Quantification of Target Ions Co^{2+} and I^- using UV-vis Spec- troscopy

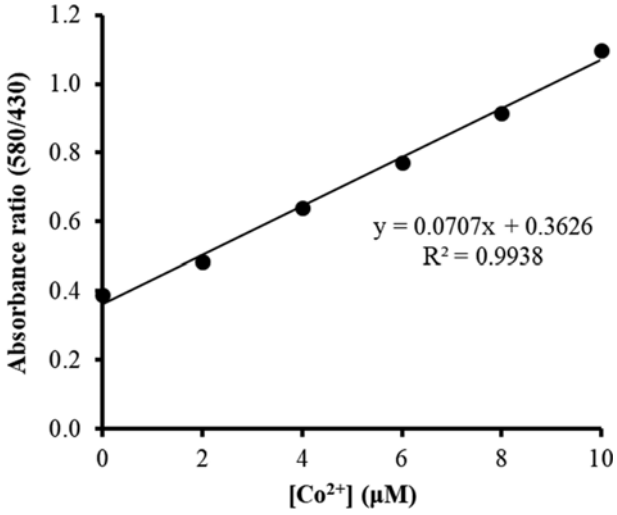

Fig. S1. Colorimetric determination of cobalt ions in water. Linear relationship of the absorbance ratio (A580/A430) of metal-Xylenol Orange complex with concentration of Co^{2+}.

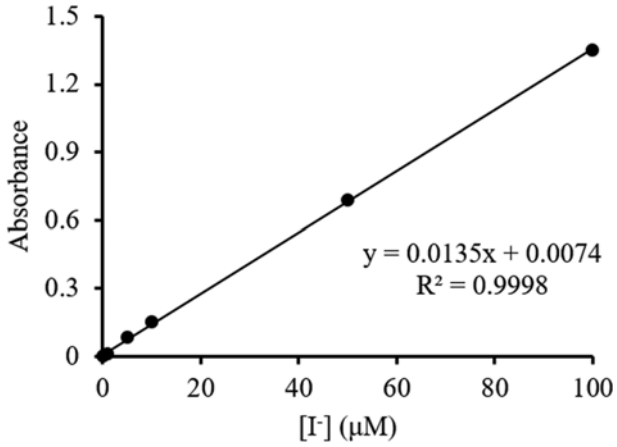

Fig. S2. Linear relationship of the absorbance at 226 nm with the concentrations of iodide (NaI) in water.

2. Preparation of Au-CAM using AuNPs and CAM

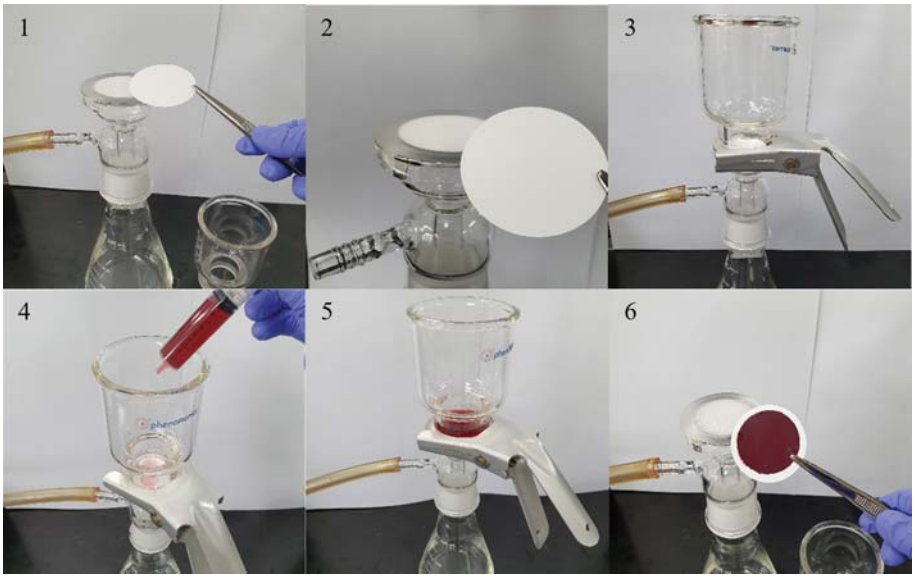

Fig. S3. Procedure for the preparation of the composite membrane (Au-CAM) via a vacuum filtration.

3. Stability of Au-CAM in Aqueous Solutions

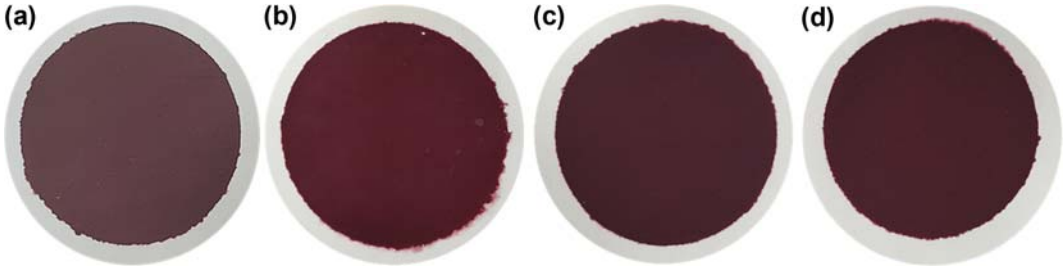

Fig. S4. (a) A photographic image of Au-CAM (diameter 47 mm). (b) A photographic image of Au-CAM in 0.1 M HCl after 1 h. (c) A photographic image of Au-CAM in 0.1 M NaOH after 1 h. (d) A photographic image of Au-CAM in 1.0 M NaCl after 1 h.

4. Adsorption Isotherm

Adsorption isotherm experiments were conducted by adding cobalt or iodide solution to NTA-Au-CAM (3.6 mg of adsorbents) in a petri dish. A concentration range of cobalt ion was ranged from 2.5 to 100 μM and that of iodide ion was ranged from 10 to 500 μM. The petri dishes were shaken gently at room temperature for 1 h to reach equilibrium. The amount of ions captured on the composite membrane under equilibrium conditions was obtained from the following equation:

$$Q_e = \frac{(C_0 - C_e)}{m} \times V \quad (1)$$

where C_0 and C_e are the initial and equilibrium concentrations of cobalt or iodide ions (mg/L), respectively; V is the volume of solution (L); m denotes the mass of the adsorbent (g).

The isotherm data obtained were fitted using the Langmuir and Freundlich models. The two typical adsorption isotherms can be expressed as:

$$\text{Langmuir equation:} \quad \frac{C_e}{Q_e} = \frac{C_e}{Q_{max}} + \frac{1}{Q_{max} K_L} \quad (2)$$

$$\text{Freundlich equation:} \quad \ln Q_e = \ln K_F + \frac{1}{n} \ln C_e \quad (3)$$

where Q_e is the adsorption capacity (mg/g), C_e is the equilibrated concentration of heavy metal ions (mg/L), Q_{max} is the saturated adsorption capacity (mg/g), and K_L and K_F refer to the affinity parameter of the Langmuir sorption constant and Freundlich adsorption capacity, respectively. 1/n is the Freundlich adsorption intensity parameter.

5. Adsorption Kinetics

The adsorption kinetics of the composite membrane was carried out by adding 3 mL of solution (for Co^{2+}: 100 μM, for I^-: 500 μM) to NTA-Au-CAM (3.6 mg of adsorbents) with shaking gen-

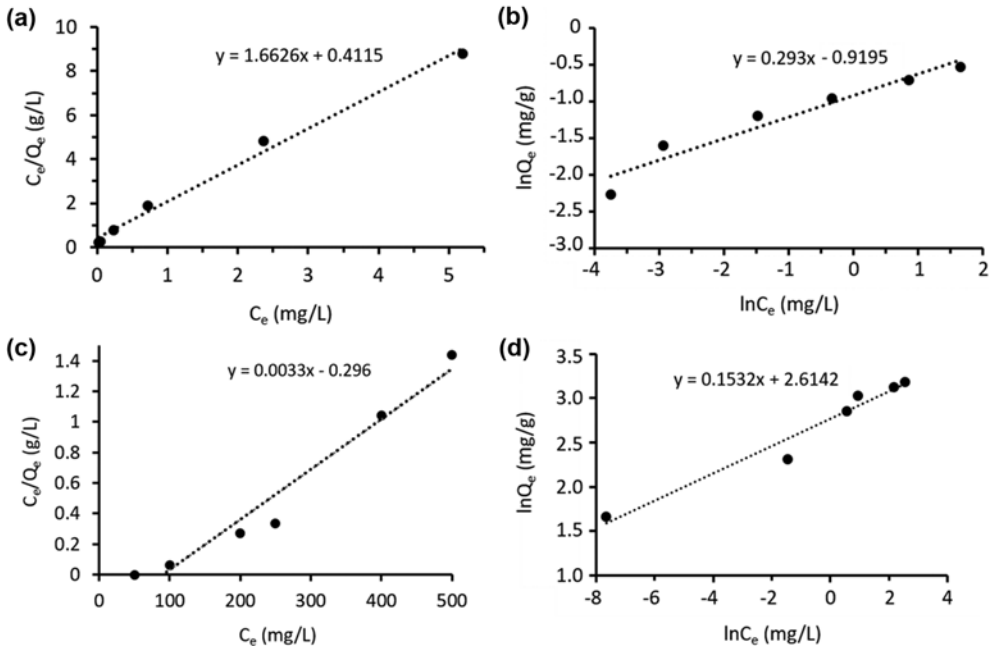

Fig. S5. Isotherms for the removal of Co^{2+} and I^- using NTA-Au-CAM. ((a) and (c)) Langmuir plot for Co^{2+} and I^- respectively; ((b) and (d)) Freundlich plot Co^{2+} and I^- respectively.

tly at room temperature for 1 h. Pseudo-first-order and pseudo-second order kinetic models were applied to interpret the adsorption kinetics to investigate desalination performance. These kinetics models are given as follows:

Pseudo-first-order kinetic model: $$\ln(Q_e - Q_t) = \ln Q_e - \frac{k_1 t}{2.303} \quad (5)$$

Pseudo-second-order kinetic model: $$\frac{t}{Q_t} = \frac{1}{k_2 Q_e^2} + \frac{t}{Q_e} \quad (6)$$

where Q_e is the adsorption capacity at equilibrium (mg/g), Q_t is the amount of ions adsorbed at time t (mg/g), k_1 is the pseudo-first-order adsorption rate constant (min^{-1}), and k_2 is the pseudo-second-order adsorption rate constant (g mg^{-1} min^{-1}). R^2 are the corresponding correlation coefficients.

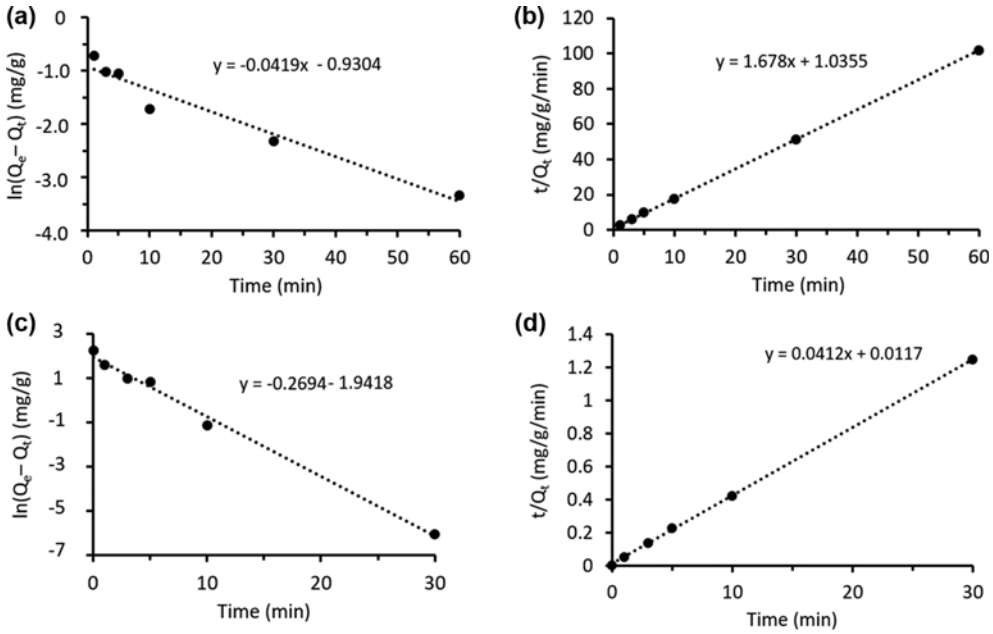

Fig. S6. ((a) and (c)) Pseudo-first order kinetic data for Co^{2+} and I^- respectively; ((b) and (d)) pseudo-second kinetics data for Co^{2+} and I^- respectively.